ABSTRACT

ZHU, YUNJIA. A Wireless Power Transfer Wearable Garment. (Under the direction of Dr. Warren Jasper).

Since the 1890's with the invention of the Tesla Coil, engineers have been designing efficient means to transmit power wirelessly. Until recently, most short range wireless power transfer devices were designed and fabricated with rigid coils or antennas. My thesis introduces a unique method which embeds a coil into a wearable weft knitted garment to receive electrical power from a power source. The wireless power transfer technology is based on resonant impedance matching with a flexible (non-rigid) coil. Two port network analysis predicts that 30% power transfer efficiency can be achieved over a 20cm distance for an optimally tuned circuit. A knitted garment was designed and fabricated out of cotton and stainless steel yarns which experimentally verify the theory.

A Wireless Power Transfer Wearable Garment

by
Yunjia Zhu

A thesis submitted to the Graduate Faculty of
North Carolina State University
in partial fulfillment of the
requirements for the degree of
Master of Science

Textile Engineering

Raleigh, North Carolina

2017

APPROVED BY:

_____	_____
Dr. Warren Jasper Committee Chair	Dr. Jeffrey Joines
_____	
Dr. David Ricketts	

DEDICATION

To my family and friends.

BIOGRAPHY

Yunjia Zhu was born in 1992 in Wuxi, Jiangsu, China. He received his bachelor degree in textile engineering in Jiangnan University in 2015. He came to NCSU as a 3+X student in 2014 and he became a master student in textile engineering in 2015.

ACKNOWLEDGMENTS

First and foremost, I would like to thank to Dr. Jasper who gave me great ideas on my thesis and helped on my thesis research. I would like to thank to Dr. Ricketts and his student William Harris who helped me a lot in my thesis experiment. I would like to thank to Tyler Henson for his help in making knitted garment. Secondly, I would like to thank to my friends I met in US. Finally, I would like to thank to my family for love and support.

TABLE OF CONTENTS

LIST OF TABLES

LIST OF FIGURES

CHAPTER 1 LITERATURE REVIEW

1.1 Near field wireless power transfer

The earliest wireless power transfer experiment were carried out by Nicola Tesla. During his experiments, he designed two coupled coils: one in the transmitter circuit and another in the receiver circuit. By incorporating a capacitor into the circuit, Tesla was able to build an 'oscillation transformer' [1] . An oscillation transformer is comprised of two coils that are tuned to resonate at the same frequency, which is also called magnetic resonate coupling.

1.1.1 Wireless power transfer in medical device

Wireless power transfer has been used to transfer energy to medical implants for several decades. In 1977, a group at the Engineering Design Centre of Case Institute of Technology investigated a method to power an implant medical device with a radio frequency [2]. The transmitter coil was driven by a radio frequency powered from an amplifier. The receiver coil picked up the radio frequency power (AC) and converted it into DC power which powered the device. Ko also introduced a procedure for designing the transmitter and receiver coils to reach the optimum power delivery efficiency. Their idea was to determine the optimum resistance of the receiver coil in order to make sure it was matched to the load. Their transmitter coil diameter was 2 inches and receiver coil was 0.5 inches. Ko achieved a coil efficiency of 39% over 1 inch, which is the ratio of the power delivered into the load to the power delivered into transmitter coil.

In 2008, Si et. al. [3] presented a method to receive power from a transmitter circuit by tuning the circuit at its resonant frequency. Figure 1 illustrates a wireless power transfer configuration for a LVAD (left ventricular assist device). In their design, a receiver coil is implanted under the skin to power a device such as an artificial heart. The primary coil was placed outside of the patient's body and was connected to a power supply.

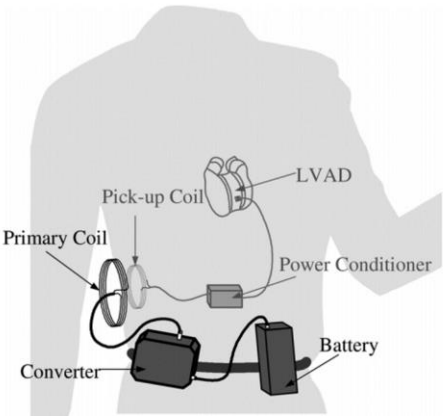

Figure 1 Wireless power transfer configuration for LVAD [3]

Wireless power transfer technology is based on changing the operating frequency, where the power efficiency is a function of the operational frequency. The pick-up circuit on the receiver side is designed to match the AC frequency transferred from the transmitter side.

1.1.2 Wireless power transfer in wireless charging

Wireless charging is a popular application of wireless power transfer technology [4], featuring a contactless battery charger that employs a pair of printed circuit board windings. Fig. 2 illustrate the configuration of a pair of neighoring printed circuit boards.

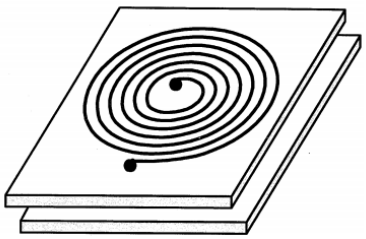

Figure 2 Neighboring PCB [4]

This wireless charging device is designed to charge batteries in a cell phone. The transmitter coil is placed on the desk-top (the primary side of charger), while the secondary side of the charger (located inside the smart phone) contains a printed circuit board wingding and a lithium-ion battery. The pair of windings can be considered as a transformer with a leakage inductance. Alternating current flows into the PCB windings in the primary side that generates an alternating magnetic field which induces a voltage across the PCB winding in the secondary side. Such a configuration can charge a cell phone with 800mA and 4V or 400mA and 8V with a power transfer efficiency of around 50%.

1.2 Maximum Power Transfer and Power efficiency

To consider the wireless power transfer efficiency, the maximum power transfer theorem must be applied. The maximum power transfer theorem states that "maximum power is transferred when the internal resistance of the source equals the resistance of the load." It was put forward by Moritz von Jacobi around 1840 and is also referred as Jacobi's Law.

This theorem can be extended to alternating current circuits that including reactance (complex impedances) . In alternating current circuits, maximum power transfer occurs when the load impedance is equal to the conjugate of the source impedance. Fig. 3 is the fundamental circuit of power transfer. [5]

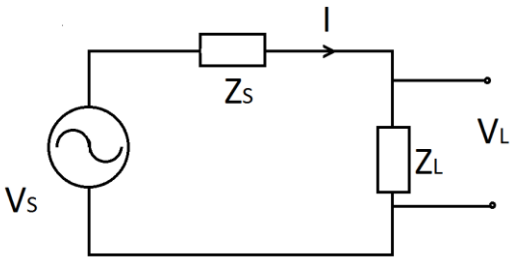

Figure 3 Power transfer circuit

Where $Z_s = R_s + X_s$,$Z_L = R_L + X_L$, and R_s and R_L are the real part of Z_s and Z_L, X_s and X_L are the imaginary part of Z_s and Z_L

From Ohms law,

$$|I| = \frac{|V_s|}{|Z_s + Z_L|} \tag{1}$$

The power delivered to the load P_L can be obtained from:

$$I_{RMS} = \frac{\sqrt{2}}{2} I \tag{2}$$

$$P_L = {I_{RMS}}^2 R_L = \frac{1}{2} I^2 R_L = \frac{1}{2} \cdot \left(\frac{|V_s|}{|Z_s + Z_L|} \right)^2 \cdot R_L \tag{3}$$

$$P_L = {I_{RMS}}^2 R_L = \frac{1}{2} \cdot \frac{|V_s|^2}{(R_S + R_L)^2 + (X_S + X_L)^2} \cdot R_L \tag{4}$$

To maximize P_L, minimize $(R_S + R_L)^2 + (X_S + X_L)^2$, by letting $X_S + X_L$equal to 0 since the reactance can be positive or negative. The resistance, however, must be positive.

The power delivery to the load P_L becomes

$$P_L = \frac{1}{2} \cdot \frac{|V_s|^2}{(R_S + R_L)^2} \cdot R_L = \frac{1}{2} \cdot \frac{|V_s|^2}{\frac{{R_S}^2}{R_L} + 2R_S + R_L} \tag{5}$$

When $R_L = R_S$, the denominator $\frac{{R_S}^2}{R_L} + 2R_S + R_L$ is a minimum which maximizes P_L. For a complex impedance, Z_s and Z_L become complex conjugates ($R_S = R_L, X_S = -X_L$) to maximize power transferred to the load. The maximum power delivered to the load P_{max}

$$P_{max} = \frac{1}{2} \cdot \frac{|V_s|^2}{4R_S} \tag{6}$$

The ratio of the power transferred to the load to the theoretical maximum power delivered is

$$\frac{P_L}{P_{max}} = \frac{4R_S}{\frac{{R_S}^2}{R_L} + 2R_S + R_L} = \frac{4}{\frac{R_S}{R_L} + \frac{R_L}{R_S} + 2} \tag{7}$$

The efficiency η is definite as:

$$\eta = \frac{R_L}{R_S + R_L} \tag{8}$$

As show in Figure 4, the condition of maximum power transfer does not result in maximum efficiency, as it only results in 50% of power transfer efficiency from Figure 4.

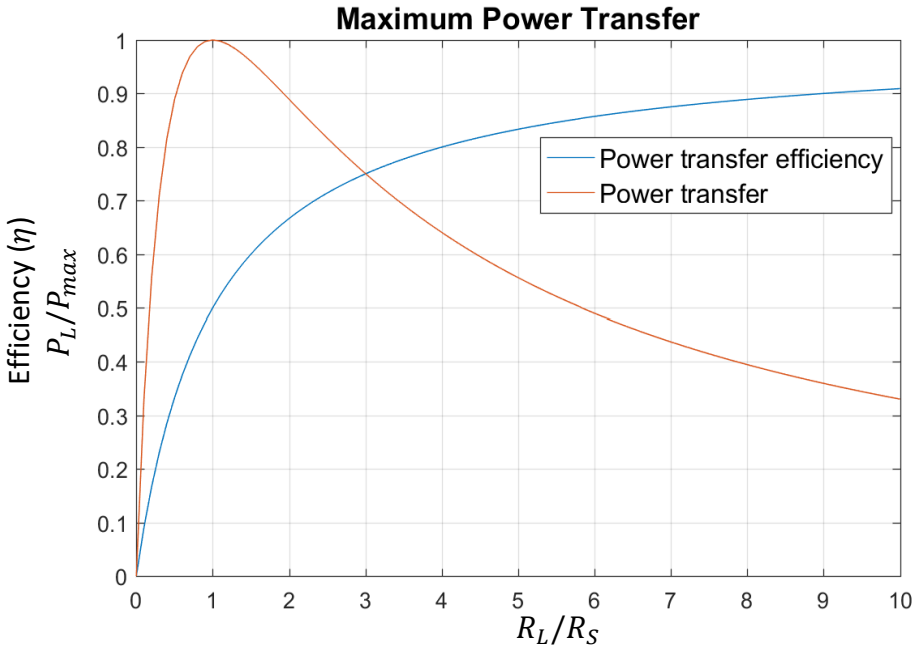

Figure 4 Maximum power transfer

If R_L is much larger than R_S, then η approaches 100%. However, in this situation, almost no power can be delivered to the load. Maximum power transfer efficiency and maximum efficiency cannot be achieved at the same time. For low power applications, such as implant medical devices, the maximum power transfer theorem is preferred, while for high power applications, such as charging electronic cars, the maximum power efficiency is more important [6].

1.3 Impedance matching

The maximum power transfer theorem states that if the load impedance and the source impedance are conjugated matched, then the maximum power can be transferred. Impedance matching methods are used to transform impedances to an ideal value to make sure the source impedance and the load impedance are conjugate matched. The impedance matching method is widely used in many wireless power transfer applications.

1.3.1 L matching network

A resister can be transformed to any resistive value by using a LC transforming circuit in two steps. [7]

(1) Use a series (shunt) reactive element to transform a smaller (larger) resistance up (down) to a larger (smaller) value with a real part equal to the desired resistance value.

(2) Use a shunt (series) reactive element to resonate with (or cancel) the imaginary part of the impedance that results from step 1.

Figure 5 illustrate the matching network (X_S and X_L) to matching load (R_L) to the source (R_S).

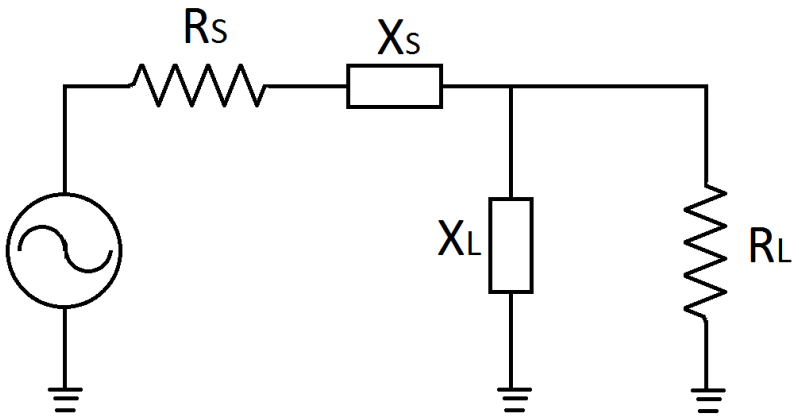

Figure 5 L Impedance matching for R_S<R_L

Impedance of X_L parallel with R_L :

$$\frac{R_L \cdot (jX_L)}{R_L + jX_L} = \frac{R_L {X_L}^2}{{R_L}^2 + {X_L}^2} + j\frac{X_L {R_L}^2}{{R_L}^2 + {X_L}^2} \tag{9}$$

Impedance of X_s series with R_s should be the complex conjugate of impedance of X_L parallel with R_L.

$$\frac{R_L {X_L}^2}{{R_L}^2 + {X_L}^2} + j\frac{X_L {R_L}^2}{{R_L}^2 + {X_L}^2} = R_s - jX_S \tag{10}$$

$$\frac{R_L {X_L}^2}{{R_L}^2 + {X_L}^2} = R_s, \frac{X_L {R_L}^2}{{R_L}^2 + {X_L}^2} = X_S \tag{11}$$

Solve for X_S and X_L:

$$\frac{R_S}{R_L} = \frac{1}{\left(\frac{R_L}{X_L}\right)^2 + 1} \tag{12}$$

$$-\frac{X_S}{R_s}=\frac{R_L}{X_L} \tag{13}$$

$$X_S=\pm R_S\cdot\sqrt{\frac{R_L}{R_S}-1} \tag{14}$$

$$X_L=\mp\frac{R_L}{\sqrt{\frac{R_L}{R_S}-1}},R_L>R_S \tag{15}$$

Positive or negative X_S and X_L means it will be inductive or capacitive. X_S and X_L always have the opposite sign. For the situation where $R_s > R_L$, the derivation is similar.

1.4 Wireless power transfer technology with impedance matching

Generally, two types of systems are used in wireless power transfer: two-coil systems and four-coil systems. Most of them can be considered as using different impedance matching methods. [8]

In a four-coil system [9] shown in Figure 6, two resonator coils are added to match the source and the load impedance. Coil A in the transmitter circuit is connected to the power source and is coupled inductively to coil S in the oscillation circuit with coupling factor K_s. The coil B in receiver circuit is connected to a resistive load and is coupled inductively to coil D in the oscillation circuit with coupling factor K_d. The two coils in the oscillating circuit are also coupled with coupling factor K. All these coils are resonating at the same frequency.

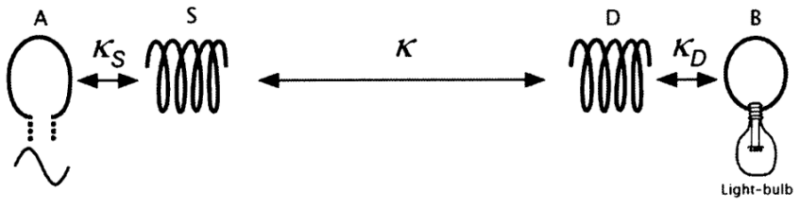

Figure 6 Experimental setup in four-coil wireless power transfer system [9]

Cheo [10] took a slightly different approach by using a simple equivalent-circuit model shown in Figure 7.

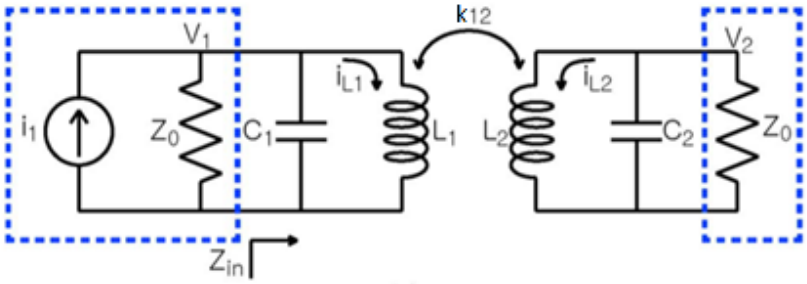

Figure 7 Circuit schematic for mutual inductance between two coils [10]

$$M_{12} = k_{12}\sqrt{L_1 L_2} \tag{16}$$

$$i_1 = \frac{V_1}{Z_0} + j\omega C_1 V_1 + i_{L_1} \tag{17}$$

$$V_1 = j\omega L_1 i_{L1} + j\omega M_{12} i_{L_2} \tag{18}$$

$$0 = \frac{V_2}{Z_0} + j\omega C_2 V_2 + i_{L_2} \tag{19}$$

$$V_2 = j\omega L_2 i_{L2} + j\omega M_{12} i_{L_1} \tag{20}$$

The equivalent circuit is shown in Figure 8.

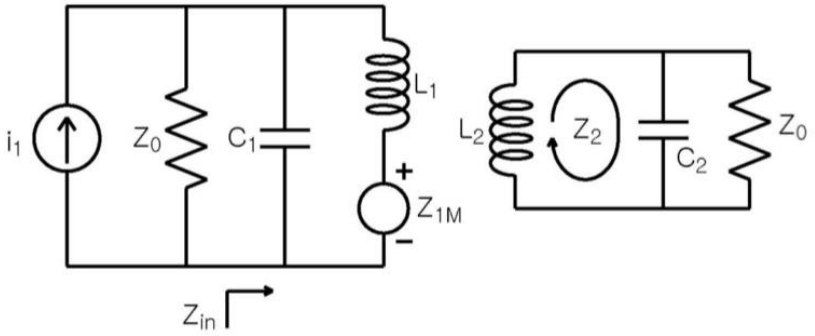

Figure 8 Compensation sources used to represent the effect of mutual inductance [10]

$$Z_{1M} = \frac{\omega^2 {M_{12}}^2}{Z_2} \tag{21}$$

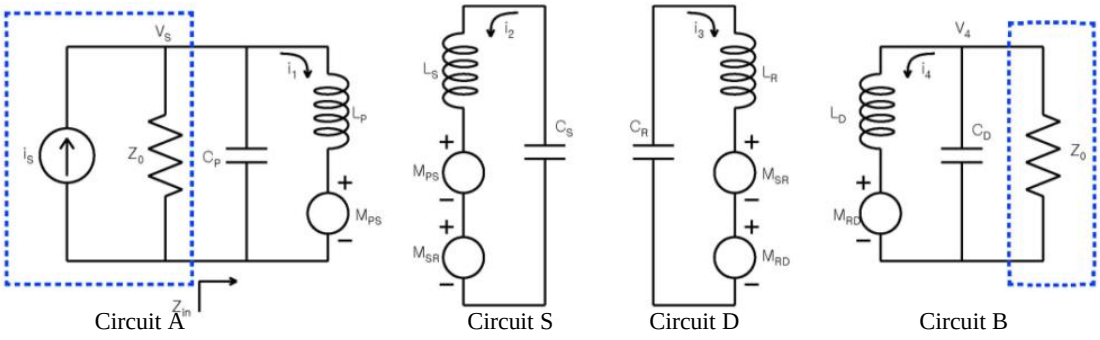

Figure 9 Equivalent circuit of four-coil system

Figure 9 is the equivalent circuit of the four-coil system. Neglecting the cross-coupling terms (coil A to coil D, coil S to coil B, coil A to coil B), each circuit can act as a compensation source with some impedance in its coupled circuit. For example, circuit B acts like a source with some impedance in coil D and the impedance is related to the coupling factor and all the elements in coil B (load resistance and coil inductance). Circuit S, circuit D and circuit B can

be represented by a source in circuit A. The equivalent impedance varies with the coupling factor K, K_s and K_D, where the coupling factors are changing with the distance between the two coupled coils. It is therefore easy to change the equivalent impedances by adjusting the distances between the coils. The maximum power transfer theorem and the efficiency theorem can be applied to achieve the desired power transfer efficiency.

The four-coil system experiment [9] transferred 60 watts with a 40% efficiency over distances more than 2 meters. Theoretically, impedance matching with a coupled oscillating circuit is lossless. In reality, the resistive part of the oscillating circuit always results in power loss. Using coils with a high Q factor in the oscillating coil will increase the power transfer efficiency.

In a two-coil system, different types of impedance matching techniques are used. A feedback analysis has been used to maximizing the power transferred to the load [11]. Figure 10 illustrates a two-coil system powering a medical implant.

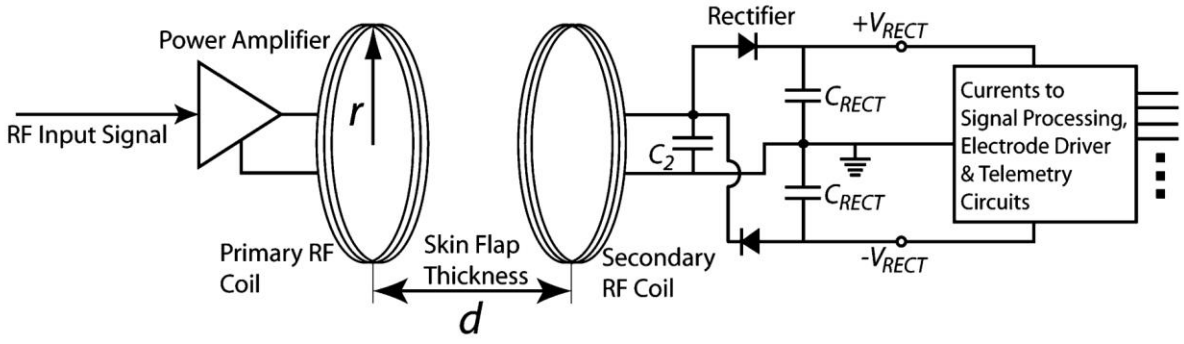

Figure 10 Two-coil system powering implant [11]

A radio-frequency power amplifier drives the transmitter (primary) coil. In the receiver circuit, the radio-frequency signal is rectified and used to power the implant device circuit. The major difference in this technique is that it uses feedback analysis to maximize the power delivered to the load. The power consumed in the implant circuit is depend upon the power supply in the transmitter circuit. In the implant device, the radio-frequency power will be delivered across the skin and dissipated into the receiver circuit. The voltage gained in the receiver coil is related to the distance "d" between the two coils, which varies with different patients. Feedback analysis is used to figure out the voltage ratio of V_1 (input power) and V_2 (output power). Figure 11 shows a block diagram for coupled resonators.

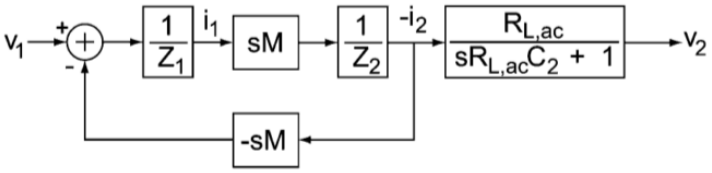

Figure 11 Feedback diagram for coupled resonators [11]

From Figure 11, the transfer function can be written as:

$$\frac{v_2(s)}{v_1(s)} = \left(\frac{L(s)}{1 - L(s)}\right)\left(\frac{1}{sM}\right)\left(\frac{R_L}{sC_2R_L + 1}\right) \tag{22}$$

From the feedback diagram, the primary coil transfer efficiency can be derived in the terms of the Q factor of the transmitter coil and receiver coil, as well as the coupling factor between the two coils. The power delivered to the receiver circuit can be split into two parts: the

power delivered to the load network and the power dissipated in the parasitic resistance in the receiver coil.

The ratio of the power delivered to the power dissipated is related by the Q factor of the receiver coil and load. The net power efficiency function is related to the transmitter circuit transfer efficiency and the power ratio in the secondary circuit. To achieve the maximum efficiency, the optimal load can be determined by differentiating of the net power efficiency function. The maximum power transfer efficiency with an optimal load is:

$$\eta_{max} = \frac{k^2 Q_1 Q_2}{(kQ_1 + 1)(kQ_2 + 1)} \tag{23}$$

whereQ_1 and Q_2 are the quality factor and k is the coupling factor of two coils. Q_1 equals to the ratio of reactance to resistance of primary coil. Q_2 equals to the ratio of reactance to resistance of secondary coil.

$$Q_1 = \frac{\omega L_1}{R_{S1}} \ , \ Q_2 = \frac{\omega L_2}{R_{S2}} \tag{24}$$

Silay [12] introduced a method to select an optimal load that maximizes the power transfer efficiency. From the circuit diagram shown in Figure 12.

$$R_{Load,opt} = \frac{Q_2 R_{s2} \sqrt{\left(Q_2{}^2 + 1\right)(R_{s1} + R_{src}) + k^2 Q_1 Q_2 R_{s1}}}{\sqrt{R_{s1} + R_{src} + k^2 Q_1 Q_2 R_{s1}}} \tag{25}$$

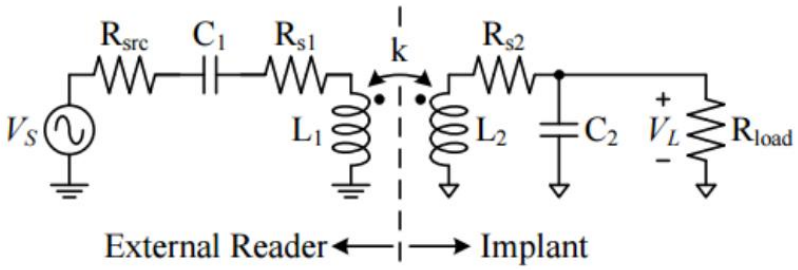

Figure 12 Circuit diagram of biomedical implant [12]

A matching network is added between the transmitter coil and the rectifier circuit to match the load impedance. In their example, the input impedance of the rectifier circuit is 87.25 - j10.35 Ω, while the optimal load is 20Ω. The matching network is designed to match the impedance to 20Ω. The experimental data shows a matching network can improve the efficiency from 24.28% to 32.52%.

1.5 Antenna and wearable garments

The most common antennas are comprised of coils of conductive materials such as copper or other low resistance metals, and are therefore rigid compared to the hand of apparel garments. It is difficult to combine a rigid element with the flexible garment. Several methods have been used to achieve this.

A wireless body-centric communication system based on RFID technology is introduced in [13]. The system is comprised of physiological sensors (sensors to measure blood pressure, temperature and so on), connected to a computer with a wireless antenna for transmission

and reception of data. Wearable radio frequency identification tag antennas operate in the 860MHz to 960MHz band. The RFID tag antenna is easily integrated into garments to enable wireless communication at any time. The mobile system can transfer data and give range of power to implanted sensors wirelessly. Figure 13 shows the approach of a wearable antenna and an implanted antenna. A wearable antenna is attached on a flexible platform that is coupled to an implanted antenna inside the body connected to the sensor to receive and transmit data.

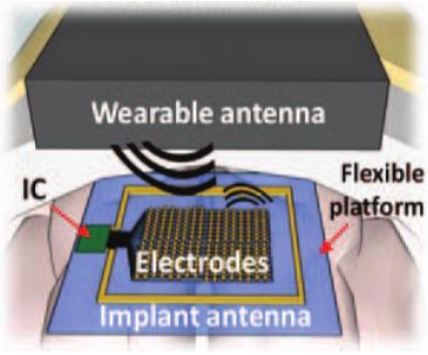

Figure 13 Wearable antenna and implanted antenna [13]

A wearable embroidered RFID tag is durable, flexible and can be easily attached or embedded in cloth. It can be fabricated by sewing conductive thread onto fabric. [14]. Figure 14 shows the embroidered tag on front side and back side.

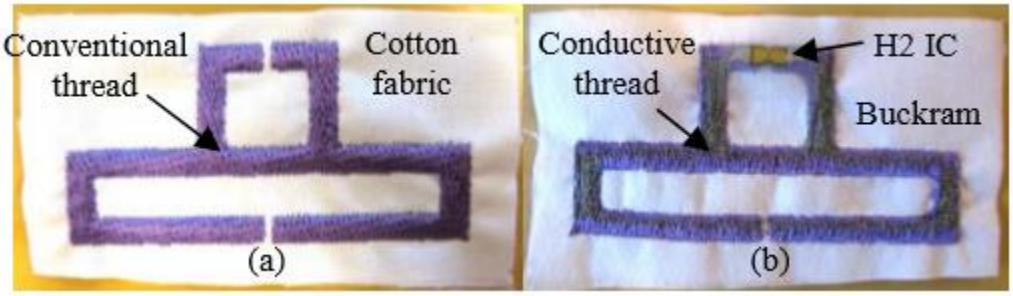

Figure 14 Embroidered RFID tag [14]

A commercial conductive thread is used to sew along the loop forming a spiral line. Figure 15 shows the embroidered antenna made from conductive thread.

Figure 15 Embroidered antenna [13]

Wearable antennas can also be used to receive power in addition to data. Instead of using physical wires, they are made stretchable through the addition of a thin layer of a ferroelastomeric material [15]. The deformable electronic system is comfortable to the skin and clothing. A stretchable ferroelastomer backplane is added to the ridged ferrite on the transmitter side. The stretchable ferroelastomer backplane is used to restrict the magnetic energy and improve the coupling between the two coils. The ferroelastomer backplane is a composite, which consists of magnetic particles at a low volume fraction in the elastomer.

The mechanical property is dominated by the polymer matrix due to the low volume fraction. A liquid metal, galinstan, has been used to fabricate a 5-turn inductor. The same geometry is used in the model of rigid coil which is made from enamel-coated copper. Figure 16 shows a liquid metal 5-turn inductor on a stretchable backplane next to a rigid coil inductor on a rigid backplane. Figure 17 shows magnetic field coupling between the two coils through the backplane.

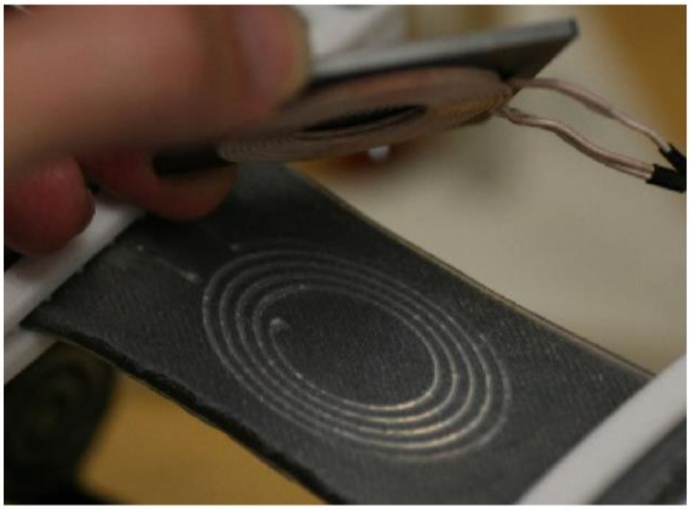

Figure 16 Inductor on stretchable backplane [15]

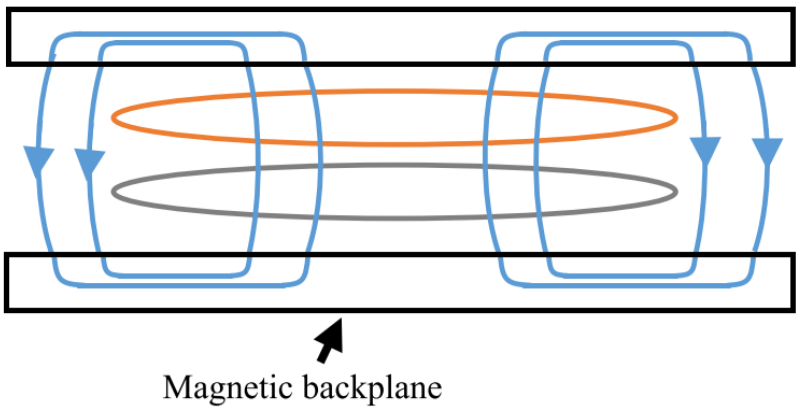

Figure 17 Magnetic field between two coils [15]

Virili [16] introduced wearable electronic modules on textiles based on an antenna design that was magnetically coupled to the active circuitry. The antenna based textile material operated in a frequency band of 2.4000-2.4835 GHz for wearable electronics and body-centric communications systems. The primary antenna was made from Flectron™ and black foam and the second antenna is made from Dupont Pyralux™ (See Figure 18). A bi-adhesive tape insulates the two antennas from shorting.

The sewing patterns mimicked an RFID tag antenna [17] . The wearable RFID tags were integrated into the clothing. The embroidery tag antennas were sewn by using cotton and a multifilament conductive thread. Cotton was used as a substrate, while conductive thread was used in fabricating the antenna pattern. A T-matched dipole was also sewn using conductive threads to match the input impedance. Figure 19 shows the pattern as dipoles. Figure 20 shows the embroidered pattern as a T-matched dipole.

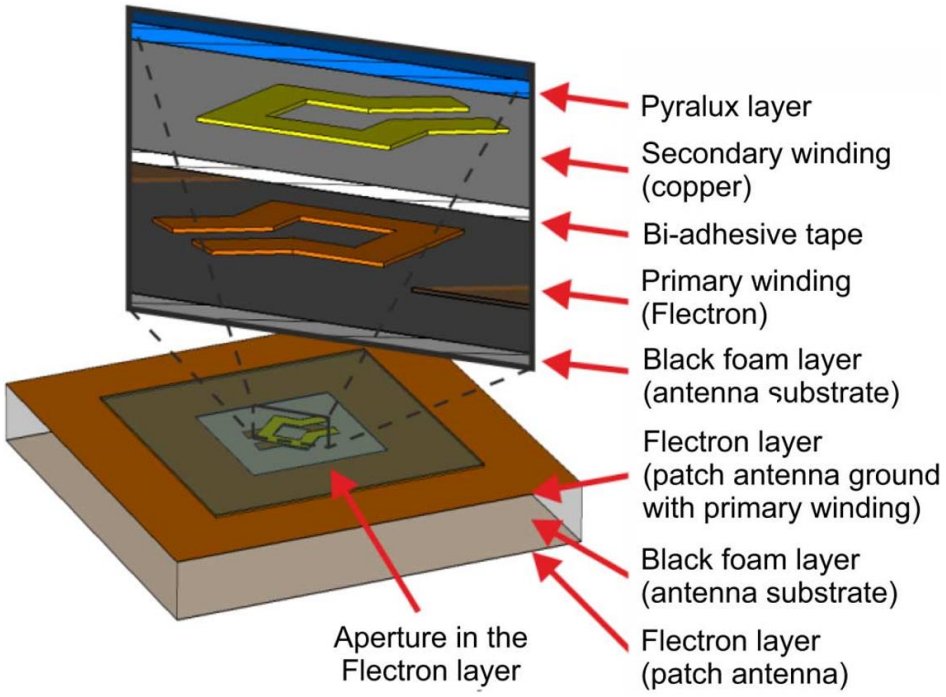

Figure 18 Wearable antennas [16]

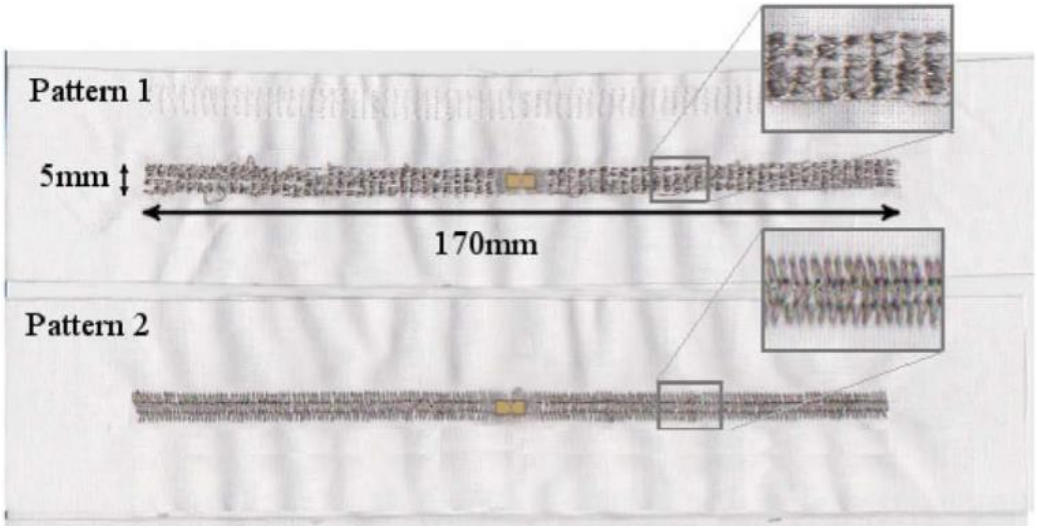

Figure 19 Embroidered dipoles [17]

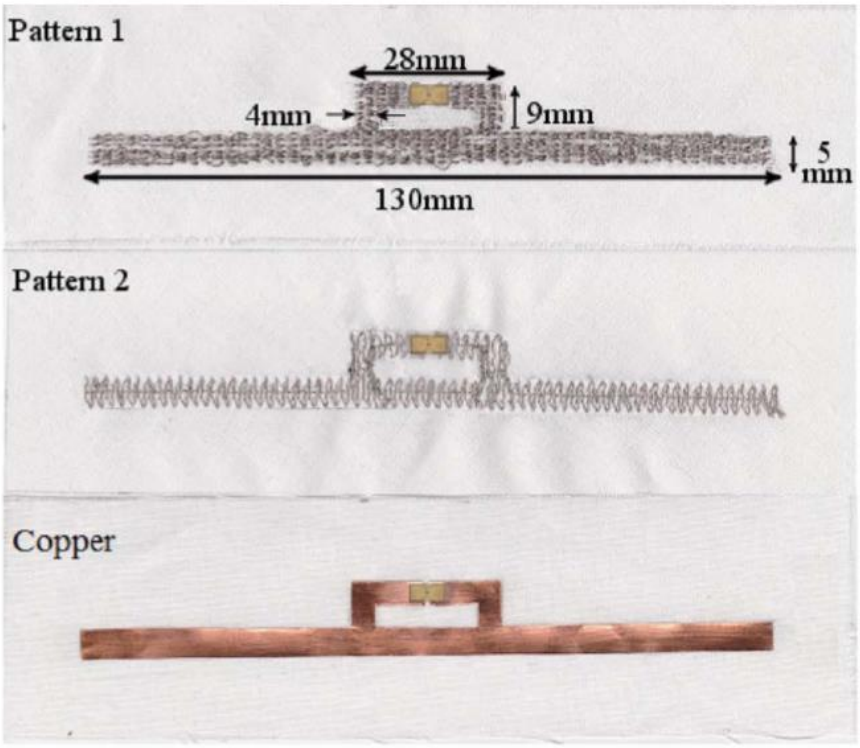

Figure 20 T-matched dipole [17]

The wearable wireless power transfer designs reviewed above all use two dimensional planar circular conductive threads to fabricate the antenna. Three dimensional helical resonant coils have also been used in wearable wireless power transfer systems [18]. The thin film cell consists of three layers, show in Figure 21. The exterior conductor layer forms an inductor that captures and generates the magnetic field. The interior layer consists of several conductive strips in parallel with the axis of the cell to form capacitors.

Figure 21 Helical resonant coil [18]

Figure 22 shows a setup of a wearable wireless power transfer system. Comprised of a single transfer system, one transmitter and multiple receiver coils that are inductively coupled. The transmitter coil is placed around the waist, and smaller receiver coils are placed around body near implanted or worn devices. The system is used to recharge or power worn or implanted devices.

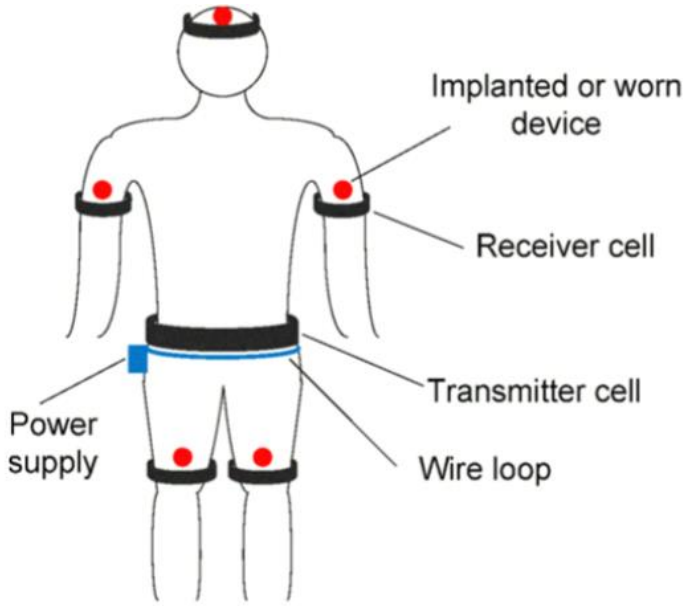

Figure 22 Wearable wireless power transfer system setup [18]

In summary, wireless power transfer technology has been proposed for almost one hundred years. Two coil impedance matched systems are commonly used. Inductive coupling is mostly used for the short range wireless power transfer. In wearable systems, this technology is used to power biomedical implants or small electronic devices. Circular conductive thread on the fabric have also been used to fabricate transmitter coils.

CHAPTER 2 INTRODUCTION

2.1 Wireless power transfer

Wireless power transfer (WPT) is designed to deliver electrical power to an electrical load without connecting the source and load with an electrical conductor. Wireless power transfer can be divided into two categories, non-radiative and radiative. Non-radiative type wireless transfer is also called near field transfer, while the radiative type is referred to as far field transfer. The difference between these two categories is the distance between the transmitter and the receiver antenna. In far field transfer, electric and magnetic fields propagate as an electromagnetic wave and the two fields are perpendicular to each other and perpendicular to the direction of wave propagation. The electromagnetic fields decay slowly as (1/r). The nearfield or non-radiative type requires the distance to be smaller than one wavelength. The magnetic field exhibits radial dependence and decays very fast as ($1/r^3$) [19]. This thesis focuses on inductive coupling which is one of the nearfield wireless power transfer techniques.

2.1.1 Inductive coupling

Inductive coupling or magnetic coupling is one of the most commonly used wireless power transfer techniques. Power is transferred between inductively coupled coils. An oscillating magnetic field is created by an AC power source in a transmitter coil. The oscillating magnetic field goes through the receiver coil and induces an AC voltage.in the receiver coil. The power is transferred from the transmitter coil to the receiver coil.

2.1.2 Resonant inductive coupling

Resonant inductive coupling is similar to inductive coupling. The difference between them is that capacitors are added into the transmitter and receiver coils to make sure they will resonate at the same frequency. Figure 23 show a basic RLC circuit. The AC power oscillates at the resonant frequency between the inductor and the capacitor. The power only dissipates through the resistor.

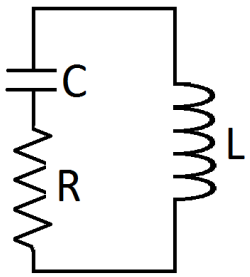

Figure 23 Example of series RLC resonate

2.1.3 Resonate frequency and Q factor

The resonate frequency ω is determined by the inductor and capacitor.

$$\omega = \frac{1}{\sqrt{LC}} \tag{26}$$

The Q factor (quality factor) is the ratio of the amount of power store in the system to the power dissipated. In an RLC circuit the Q factor is defined as:

$$Q = \frac{\omega L}{R} \tag{27}$$

A high Q factor results in a small amount power loss in the system, which implies high power transfer efficiency. This is also the reason why wireless power transfer applications prefer high frequencies. A high frequency results in the high Q, which can be seen from Eqn. (27). There are disadvantages to high frequency applications including cost and health/ safety concerns.

2.2 Knitted garment

Knitting is the most common fabric manufacturing method. In knitting, a fed yarn is converted into a new loop at each needle hook. A course or row of loops are formed by pulling new loops through the old loops. [20]

2.2.1 Warp knitting and weft knitting

There are two kinds of knitting technology: weft knitting and warp knitting. One difference between the two knitting technologies is the knitting direction. In warp knitting, yarns are knitted in the warp direction, while in weft knitting loops are knitted along a course. Figure 24 (a) and Figure 24 (b) shows the weft knitting structure on the machine. In warp knitting, the yarns are fed to the needle by separate yarn guides on the guide bar. Loop formation occurs at each needle simultaneously during one knitting cycle.

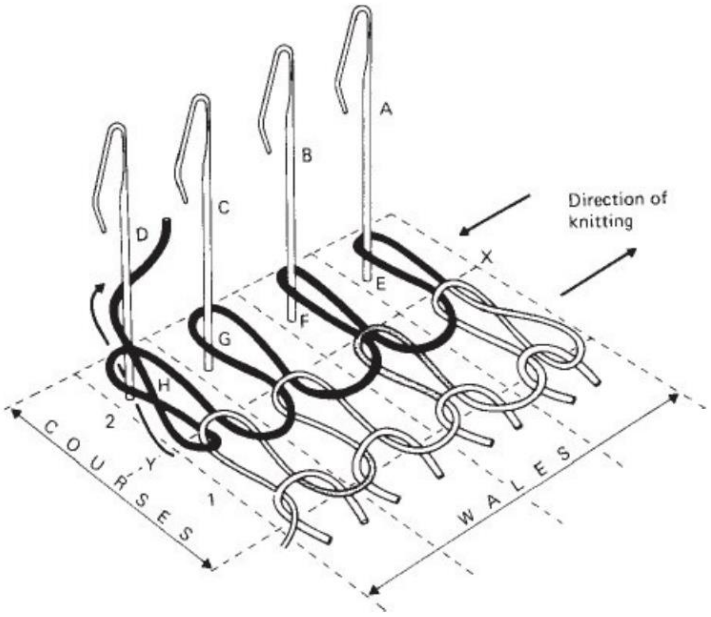

Figure 24 (a) Weft knitting [20]

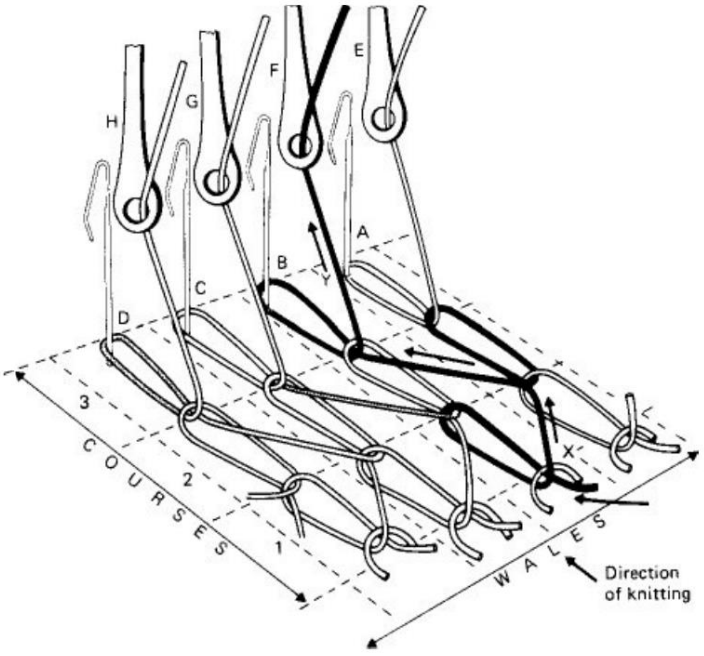

Figure 24 (b) Warp knitting [20]

2.2.2 Rib weft knitting structure

Four primary weft knitting structures are plain, rib, interlock and purl. The weft rib structure was invented in 1755. The simplest rib fabric is a 1×1 rib. One face loop wale and one back loop alternatively appear in the structure. The face loop tends to move over and in front of the back loop wale, so, the technical face appears on the both sides of the fabric unless the fabric is stretched. Figure 25 (a) shows a 1×1 rib structure knitted. where Figure 25(b) is the stretched 1×1 rib structure.

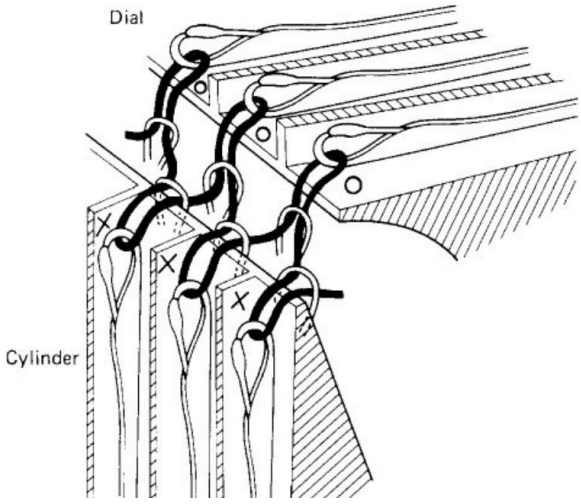

Figure 25 (a) 1×1 rib structure on machine [20]

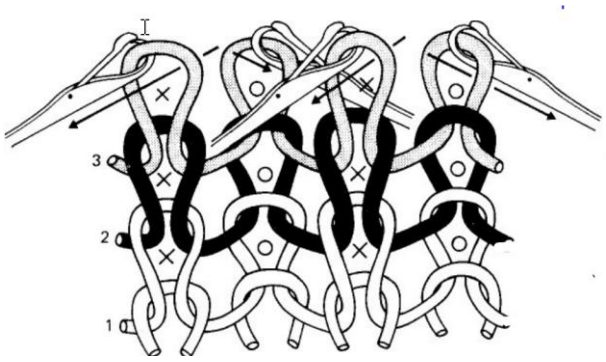

Figure 25 (b) 1×1 rib structure off machine [20]

2.2.3 Weft knitting inlay

An inlaid yarn is never formed into knitted loops in a weft knit fabric, but rather other yarns form loops around it as shown in Figure 26. In a double jersey fabric, such as a 1×1 rib, the inlaid yarns are trapped inside the face loops and back loops. This is also referred to as a tunnel inlay technique, where the inlayed yarn appears as a straight horizontal yarn inside the fabric. A fabric with an inlaid yarn lacks flexibility (and extensibility) due to the straight inlaid yarn unless the inlaid yarns themselves are elastic. Figure 26 demonstrates the simulation of the tunnel inlay (inlaid yarns in 1×2 rib structure).

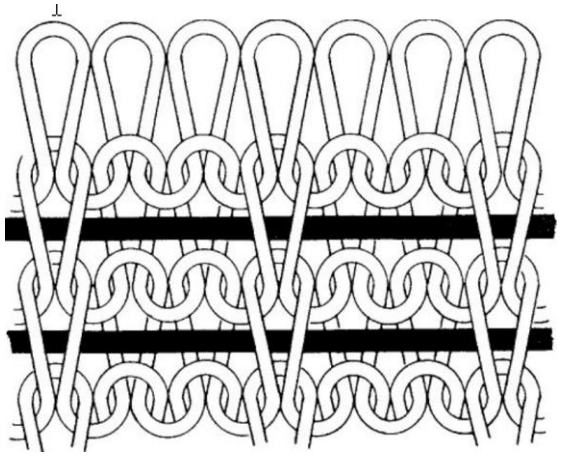

Figure 26 Tunnel inlay [20]

CHAPTER 3 EXPERIMENT

3.1 Fabricate the wearable garment

3.1.1 Conductive yarn

The conductive yarn used in our WPT knitted garment is manufactured by Bekaert Fibre Technologies. It is made of many thin stainless steel filaments twisted together to form a thick yarn. The yarn is not appropriate for our fine gage knitting machines, but can be inlayed into the garment.

Table 1 Fiber Data

Type	Tex (g/1000m)	Elongation (%)	Linear Resistivity (Ohm/m)
VN 12/4 ×275	1010	1	6.9

3.1.2 Weft knitting for garment

A wearable garment was fabricated on a Shima Seiki whole garment computerized flat knitting machine.

To incorporate the conductive yarn with the wearable garment, a tunnel inlay structure was used. In an inlay structure, the inlaid yarn is kept straight in the knitting loop. The main structure is a 1×1 rib. To fabricate the helical coil to operate as an antenna, the conductive yarn is inserted between the front wale and back wale.

A tubular-shaped rib structure garment was produced on a flat-bed knitting machine in a carefully arranged sequence. First, a single course of 1×1 rib is knitted using both needle beds (Figure 27(a)) and is then transferred off onto one single bed as shown in Figure 27(b).

The back side is knitted in a similar way. The back side is knitted using the needles on both needle beds that were not used during the previous course as shown in Figure 27(c) and then the back loops are transferred to the front bed shown in Figure 27(d). The front side and the back side of loops form one course of 1×1 rib.

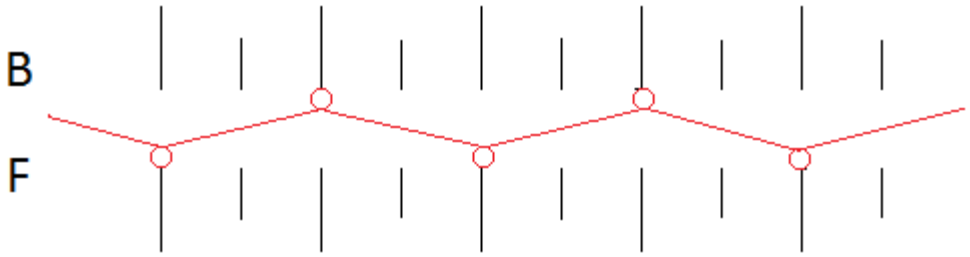

Figure 27(a) 1×1 rib knitted on two needle beds

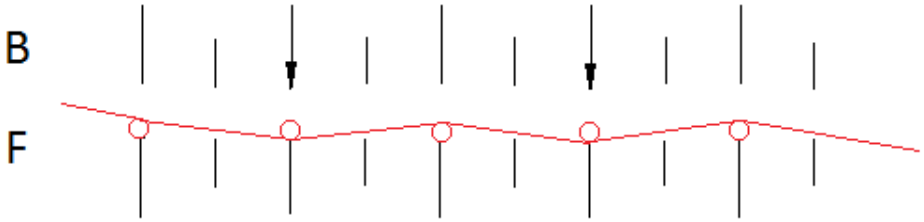

Figure 27(b) 1×1 rib knitted on two needle beds

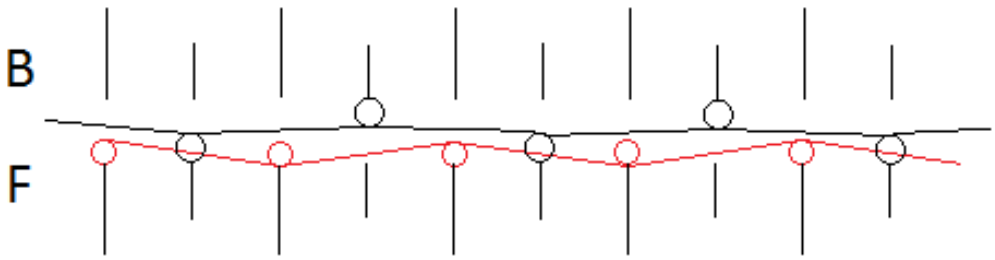

Figure 27(c) Next course knitting

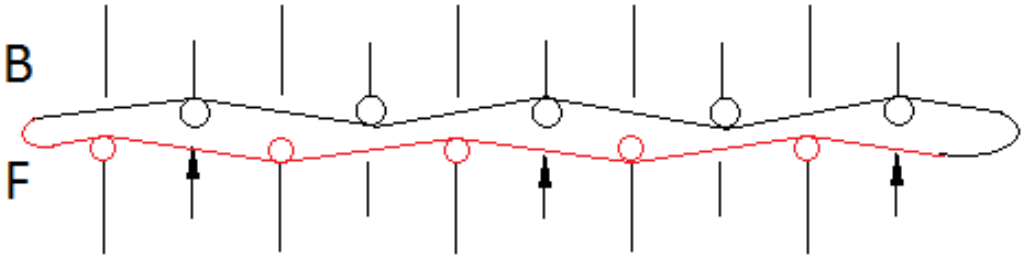

Figure 27(d) Loops transfer

After eight courses are constructed, an inlaid yarn is inserted before the loop transfer occurs as shown in the Figure 27(e). The loop transfer locks the inlay yarn between the front loops and back loops as shown in Figure 27(f).

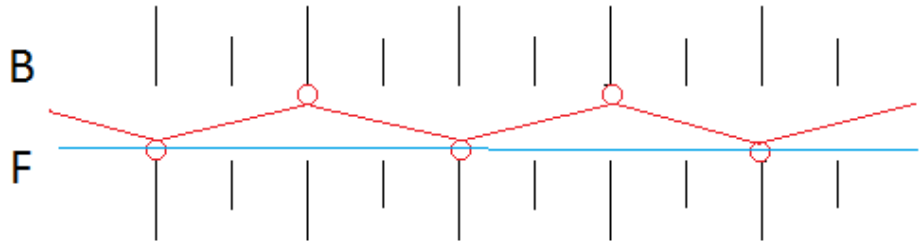

Figure 27(e) Inlay before loop transfer

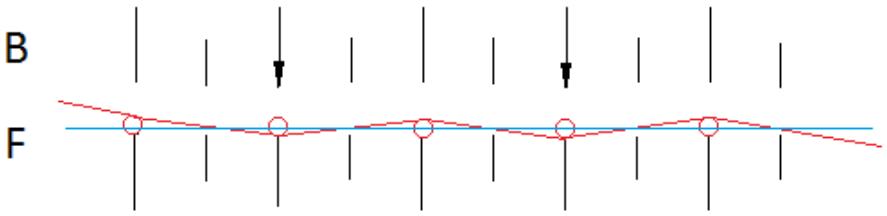

Figure 27(f) Inlay after loop transfer

The inlay creates a helical coil at the bottom of the garment. Figure 28 and Figure 29 show the inlay part in the final garment.

Figure 28 Wearable garment

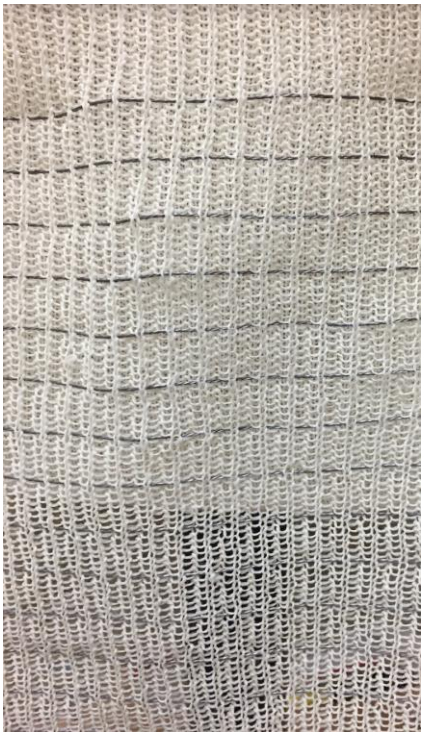

Figure 29 Inlay part in the garment

3.1.3 transmitter coil

Transmitter coil was made by winding a 12-gauge wire into a 9-inch diameter loop with 28 turns. The inductance of the coil is 260.7μH and its resistance is 0.5 ohms.

Figure 30 Transmitter coil

3.2 Experiment by VNA (Vector Network Analyzer)

3.2.1 Two port network Z parameter

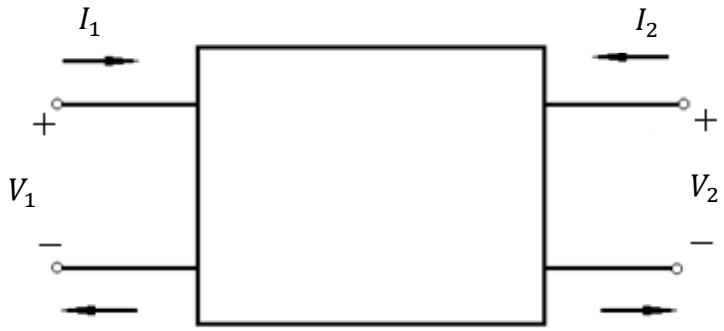

Figure 31 Two port network

As two-port network, shown in Figure 31, has four terminals. A port voltage is defined as the voltage difference between a pair of terminals with one of the terminals in the pair being the reference terminal. Port 1 is on the left side of the diagram, where the port voltage V_1 is defined. The current flow entering into the network at the top left terminal is I_1 and it is equal to the current leaving the reference terminal. [7]

The impedance parameters, or Z parameter are defined as:

$$\begin{bmatrix} V_1 \\ V_2 \end{bmatrix} = \begin{bmatrix} Z_{11} & Z_{12} \\ Z_{21} & Z_{22} \end{bmatrix} \begin{bmatrix} I_1 \\ I_2 \end{bmatrix} \tag{28}$$

3.2.2 Two port network S parameter

The scattering parameters (S parameters) are defined in terms of the traveling waves on the transmission lines attached to the each of the ports of the network as show in Figure 32.

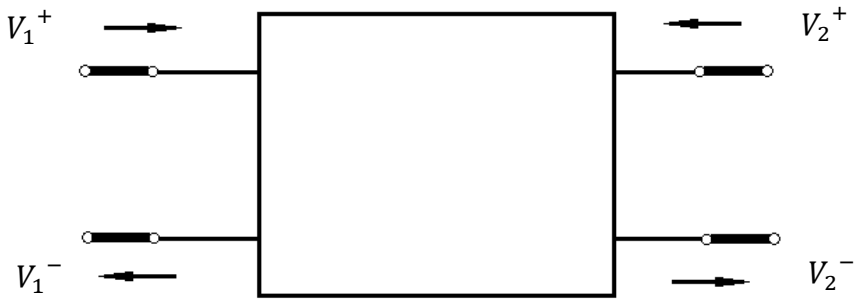

Figure 32 Two port network with transmission line

The V^+, V^-, I^+, I^- are the travelling voltages and currents measured for the forward and backward traveling waves.

$$S_{11} = \left.\frac{V_1^-}{V_1^+}\right|_{V_2^+=0} \tag{29}$$

$$S_{21} = \left.\frac{V_2^-}{V_1^+}\right|_{V_2^+=0} \tag{30}$$

$$S_{12} = \left.\frac{V_1^-}{V_2^+}\right|_{V_1^+=0} \tag{31}$$

$$S_{22} = \left.\frac{V_2^-}{V_2^+}\right|_{V_1^+=0} \tag{32}$$

3.2.3 Vector network analysis

A VNA (Vector \Network Analyzer) test system enables one to characterize the RF performance of radio frequency (RF) and microwave devices to be characterized in terms of network scattering parameters. The transmitter coil is placed beneath the garment as shown in Figure 33 and connected to a one port of the VNA.

Figure 33 Experiment with VNA

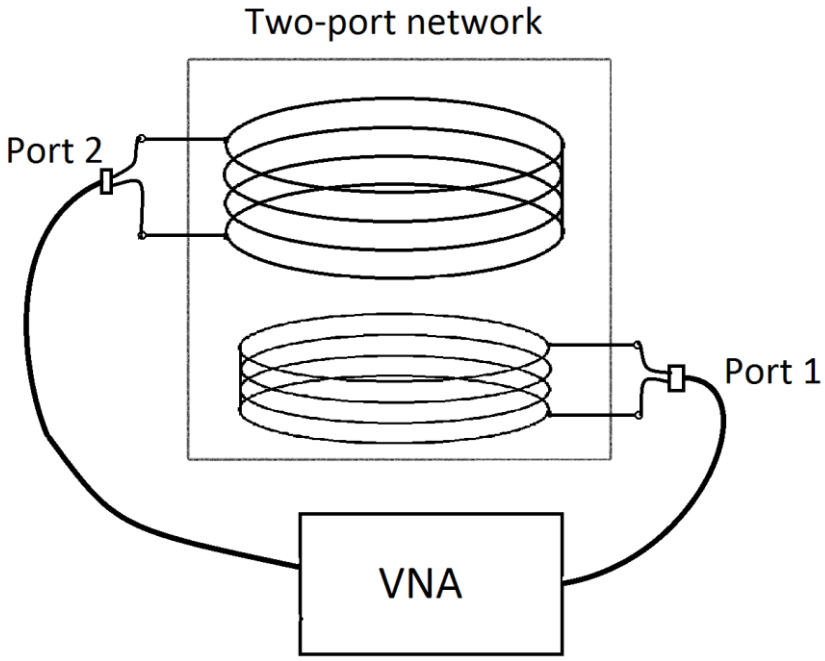

Figure 34 VNA experiment diagram

CHAPTER 4 RESULT AND DISCUSSION

The transmitter and two garments were tested in the experiment. The basic values that were measured are listed in the Table 2

Table 2 Basic values of coils

	Turns	Diameter(cm)	Resistance(ohm)	Inductance(μH)
Transmitter coil	28	23	0.5	260.7
Receiver coil (Black garment)	12	16.5	135	18
Receiver coil (White garment)	24	20	223	154

4.1 Maximum power transfer achieved by port parameter

The distance between the transmitter coil and the receiver coil (garment) is 20 cm. The S parameters are determined by VNA analysis from 300kHz to 15MHz. Figure 35 shows a plot of the $|S_{21}|$ parameter of the two garments in that frequency range.

S_{21} is a scattering parameter, as the voltage ratio between two ports is equal to $|S_{21}|$ [21].

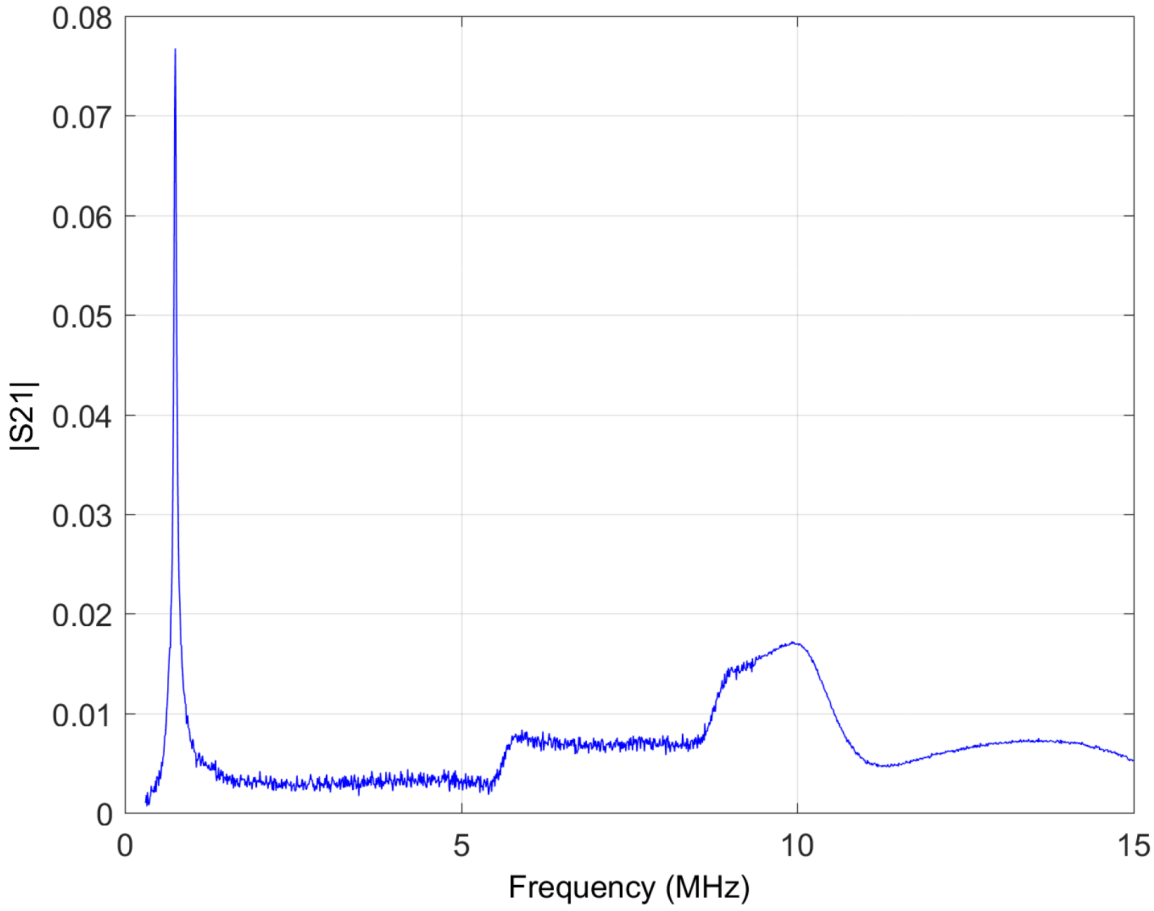

Figure 35 S_{21} two-port network

Impedance matching can improve the power transfer efficiency. The maximum efficiency that can be achieved by impedance matching is discussed in [22].

The maximum power transfer efficiency is determined from the Z parameters, which can be written in terms of the measured S parameter.

$$Z_{11} = \frac{[(1 + S_{11})(1 - S_{22}) + S_{12}S_{21}]}{(1 - S_{11})(1 - S_{22}) - S_{12}S_{21}} \tag{33}$$

$$Z_{12} = \frac{2S_{12}}{(1-S_{11})(1-S_{22}) - S_{12}S_{21}} \tag{34}$$

$$Z_{21} = \frac{2S_{21}}{(1-S_{11})(1-S_{22}) - S_{12}S_{21}} \tag{35}$$

$$Z_{22} = \frac{[(1-S_{11})(1+S_{22}) + S_{12}S_{21}]}{(1-S_{11})(1-S_{22}) - S_{12}S_{21}} \tag{36}$$

The maximum power transfer efficiency is:

$$\eta = \frac{\chi}{(1+\sqrt{1+\chi})^2} \tag{37}$$

$$\chi = \frac{|Z_{12}|^2}{Re(Z_{11}) \cdot Re(Z_{22}) - Re(Z_{12})^2} \tag{38}$$

$Re(Z)$ means the real part of Z, and $Im(Z)$ means the imaginary part of Z. The maximum power transfer efficiency η is plotted in the Figure 36.

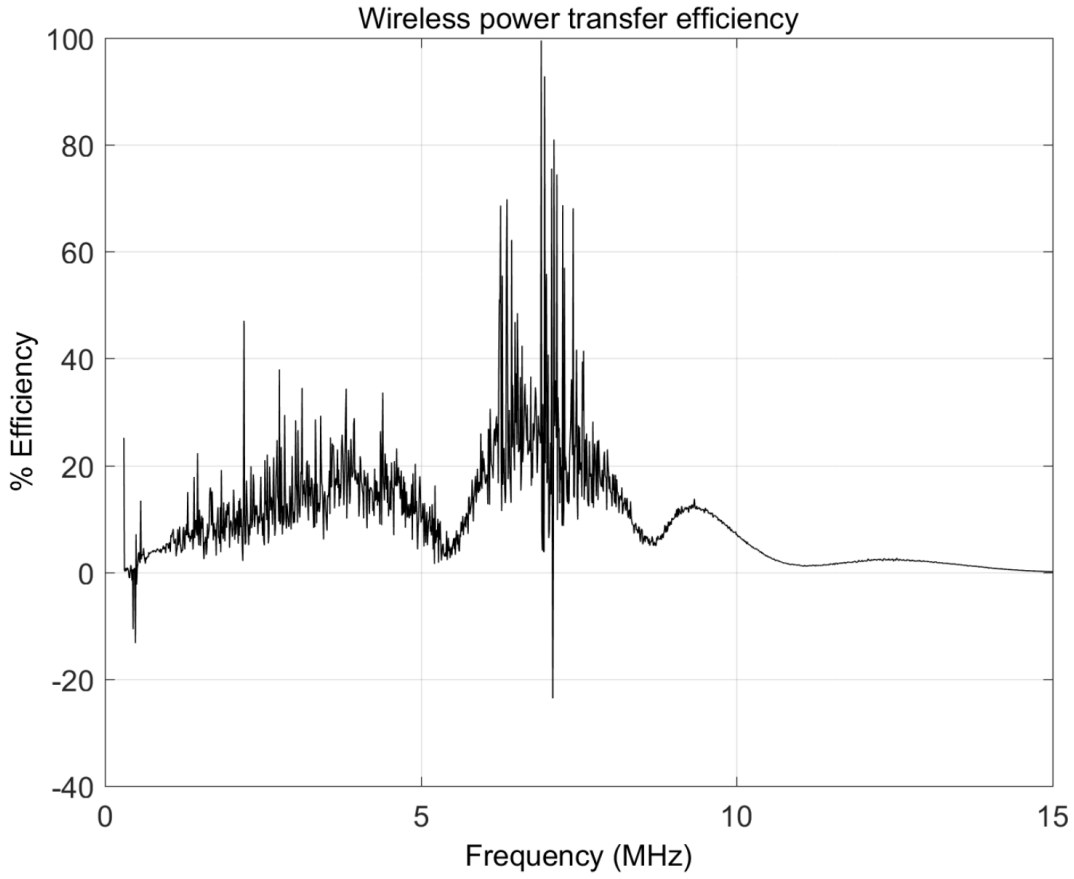

Figure 36 Maximum power transfer efficiency

As shown in Figure 36 Maximum power transfer efficiency the maximum power transfer efficiency of 30% can be achieved by choosing an optimal load at a frequency of 8MHz. The maximum power is transferred when then load on the transmitter side is equal to Z(opt).

$$Z(opt) = Re[Z(opt)] + Im\big(Z(opt)\big) \tag{39}$$

$$Re[Z(opt)] = \frac{\sqrt{(Re(Z_{11})Re(Z_{11}) + Im(Z_{12})^2)\,(Re(Z_{11})Re(Z_{22}) - Re(Z_{12})^2)}}{Re(Z_{11})} \tag{40}$$

$$Im\big(Z(opt)\big) = \frac{Im(Z_{12}) \cdot Re(Z_{12})}{Re(Z_{11})} - Im(Z_{22}) \tag{41}$$

4.2 Maximum power transfer achieved by Circuit theory

The following equation can be written by using Kirchhoff's voltage law from Figure 37

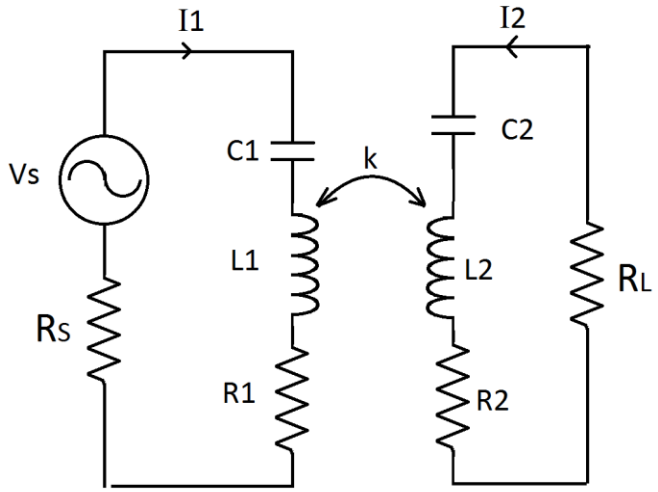

Figure 37 Equivalent circuit diagram

$$V_S = (R_S + R_1)I_1 + j\omega L_1 I_1 - j\omega M I_2 - j\frac{1}{\omega C_1} I_1 \tag{42}$$

$$-j\omega M I_1 + j\omega I_2 L_2 + (R_L + R_2)I_2 - j\frac{1}{\omega C_2} I_2 = 0 \tag{43}$$

$$M = k\sqrt{L_1 L_2} \tag{44}$$

$$\omega = 2\pi f \tag{45}$$

V_S and f are the Laplace transformed voltage and frequency of the AC source. R_S is the source resistance. k is the coupling factor of two coils. $R_1$and L_1 are the resistance and

inductance of the primary coil. $R_2$and L_2 are the resistance and inductance of the secondary coil. C_1 and C_2 are the capacitance in the primary and secondary coil.

C_1 and L_1 form the resonator. The resonate frequency f equals:

$$\omega = \frac{1}{2\pi\sqrt{L_1 C_1}} = \frac{1}{2\pi\sqrt{L_2 C_2}} \tag{46}$$

So,

$$j\omega L_1 I_1 - j\frac{1}{\omega C_1} I_1 = 0 \tag{47}$$

$$j\omega L_2 I_2 - j\frac{1}{\omega C_2} I_2 = 0 \tag{48}$$

The circuit equation simplifies to:

$$V_S = (R_S + R_1) I_1 - j\omega M I_2 \tag{49}$$

$$-j\omega M I_1 + (R_L + R_2) I_2 = 0 \tag{50}$$

The ratio of I_1 and I_2:

$$\frac{I_2}{I_1} = \frac{j\omega M}{R_L + R_2} \tag{51}$$

Substitute I_1 with I_2

$$V_S = \frac{(R_S + R_1)(R_L + R_2)}{j\omega M} I_2 - j\omega M I_2 \tag{52}$$

$$I_2 = \frac{j\omega M V_S}{(R_S + R_1)(R_L + R_2) + \omega^2 M^2} \tag{53}$$

The power transfer efficiency:

$$\eta = \frac{P_L}{P_s} = \frac{{I_2}^2 R_L}{I_1 V_s} = \frac{\omega M}{R_L + R_2} \cdot \frac{\omega M R_L}{(R_S + R_1)(R_L + R_2) + \omega^2 M^2} \tag{54}$$

$$\eta = \frac{\omega^2 M^2 R_L}{(R_S + R_1)(R_L + R_2)^2 + \omega^2 M^2 (R_L + R_2)} \tag{55}$$

$$\eta = \frac{\omega^2 M^2 R_L}{(R_S + R_1)R_L + 2R_2(R_S + R_1) + \omega^2 M^2 + \frac{\omega^2 M^2 R_2 + (R_S + R_1){R_2}^2}{R_L})} \tag{56}$$

When $\frac{d\eta}{dR_L} = 0, \eta$ goes to the maximum

$$R_L = \sqrt{\frac{(R_S + R_1){R_2}^2 + \omega^2 M^2 R_2}{(R_S + R_1)}} \tag{57}$$

4.3 Conclusion and future work

A wearable knitted garment was constructed on a Shima Seiki whole garment machine with an inlaid stainless steel yarn to demonstrate the feasibility of achieving high power transfer over moderately large distances to power wearable devices. This garment is capable of being washable and can receive power wirelessly from a powered primary coil over a distance of 20cm with a theoretical efficiency of 30%. Compared with other powering technologies, this technique can output a larger amount of power with a flexible garment without any ridge parts, such as coils.

The largest factor that affects WPT efficiency is the resistance in the secondary coil. If a conductive yarn with lower resistance be used when fabricating the garment, a higher efficiency can be easily achieved. The configuration of the secondary coil also can be

designed to achieve higher coupling factor and a higher Q factor which also can improve the power transfer efficiency.

REFERENCES

[1] N. Tesla, "Apparatus for transmitting electrical energy". US Patent 1119732, 1914.

[2] Wen H.Ko , "Design of radio-frequency powered coils for implant instruments," *Medical & Biological Engineering & computing,* pp. 634-640, 1977.

[3] P. Si, A. P. Hu, S. Malpas and D. Budgett, "A Frequency Control Method for Regulating Wireless Power to Implantable Devices," *IEEE TRANSACTIONS ON BIOMEDICAL CIRCUITS AND SYSTEM,* vol. 2, March 2008.

[4] B. Choi, J. Nho, H. Cha, T. Ahn and S. Choi, "Design and Implementation of Low-Profile Contactless Battery Charger Using Planar Printed Circuit Board Windings as Energy Transfer Device," *IEEE TRANSACTIONS ON INDUSTRIAL ELECTRONICS,* pp. 140-146, February 2004.

[5] "Maximum power transfer theorem," 17 October 2016. [Online]. Available: https://en.wikipedia.org/wiki/Maximum_power_transfer_theorem.

[6] S. Y. R. Hui, W. Zhong and C. K. Lee, "A Critical Review of Recent Progress in Mid-Range Wireless Power Transfer," *IEEE TRANSACTIONS ON POWER ELECTRONICS*, pp. 4500-4511, 2014.

[7] M. Steer, Microwave and RF Design, Raleigh: SciTech Publishing,Inc, 2010.

[8] D. S. Ricketts, . M. . J. Chabalko and A. Hillenius, "Experimental demonstration of the equivalence of inductive and strongly coupled magnetic resonance wireless power transfer," *APPLIED PHYSICS LETTERS,* 2013.

[9] A. Kurs, . A. Karali, R. Moffatt and J. D. Joannopoulos, "Wireless power transfer via strongly coupled magnetic resonances," *Science Express,* pp. 83-86, July 2007.

[10] S. Cheo, Y.-H. Kim, S.-Y. Kang, M. L. Lee, J.-M. Lee and T. Zyung, "Circuit-Model-Based Analysis of a Wireless Energy-Transfer System via Coupled Magnetic

Resonances," *IEEE TRANSACTIONS ON INDUSTRIAL ELECTRONICS*, pp. 2906-2914, 2011.

[11] M. W. Baker and R. Sarpeshkar, "Feedback Analysis and Design of RF Power Links for Low-Power Bionic System," *IEEE TRANSACTIONS ON BIOMEDICAL CIRCUITS AND SYSTEMS*, pp. 28-39, 2007.

[12] K. M. Silay, . D. Dondi, L. Larcher, M. Declercq, . L. Benini, Y. Leblebici and C. Dehollain, "Load optimization of an inductive power link for remote powering of biomedical implants," in *2009 IEEE International Symposium on Circuits and Systems*, Taipei, 2009.

[13] L. Ukkonen, L. Sydanheimo and Y. Rahmat-Samii, "Embroidered Textile Antennas for Wireless Body-Centric Communication and Sensing," in *2015 Loughborough Antennas & Propagation Conference (LAPC)*, 2015.

[14] E. Kosk, K. Koski, T. Björninen and Y. Rahmat-Samii, "Fabrication of Embroidered UHF RFID Tags," *IEEE Antennas and Propagation Society*, 2012.

[15] N. Lazaru and S. S. Bedair, "Improved power transfer to wearable systems through stretchable magnetic composites," *Applied physics A Material Science & Processing*, 2016.

[16] M. Virili, . H. Rogier, . F. Alimenti, P. Mezzanotte and . L. Roselli, "Wearable Textile Antenna Magnetically Coupled to Flexible Active Electronic Circuits," *IEEE ANTENNAS AND WIRELESS PROPAGATION LETTERS*, pp. 209-213, 2014.

[17] E. Moradi, T. Björninen, L. Ukkonen and Y. Rahmat-Samii, "Effects of Sewing Pattern on the Performance of Embroidered Dipole Type RFID Tag Antennas," *IEEE Antennas and Wireless Propagation Letters*, pp. 1482 - 1485, 2012.

[18] X. Liu, F. Zhang, A. Hackworth, R. J. Sclabassi and M. Sun, "Wireless Power transfer system design for implanted and worn devices," in *Bioengineering Conference, 2009 IEEE 35th Annual Northeast*, 2009.

[19] J. I. Agbinya, Principles of Inductive Near Field Communications for Internet of Things. Aalborg, DK: River Publishers, . ProQuest ebrary. Web., River Publishers, 2011.

[20] D. J. Spencer, Knitting Technology, Third Edition: A Comprehensive Handbook and Practical Guide, Woodhead Publishing, 2001.

[21] N. Inagaki, "Design of External Circuits for Smart Inductive Coupling between Non-Self-Resonant Small Antennas in Wireless Power Transfer Systems," in *2013 International Symposium on Electromagnetic Theory*, 2013.

[22] M. Zargham and . P. G. Gulak, "Maximum Achievable Efficiency in Near-Field Coupled Power-Transfer Systems," *IEEE TRANSACTIONS ON BIOMEDICAL CIRCUITS AND SYSTEMS*, pp. 228-246, 2012.

[23] A. K. RamRakhyani, S. Mirabbasi and M. Chiao, "Design and Optimization of Resonance-Based Efficient Wireless Power Delivery Systems for Biomedical Implants," *IEEE TRANSACTIONS ON BIOMEDICAL CIRCUITS AND SYSTEMS*, pp. 48-62, 2011.

[24] K. M. Silay, C. Dehollain and M. Declercq , "Improvement of Power Efficiency of Inductive Links for Implantable Devices," in *Research in Microelectronics and Electronics*, 2008.